ELSEVIER

Journal of Nuclear Materials 241–243 (1997) 861–866

journal of nuclear materials

ICRF wall conditioning at TEXTOR-94 in the presence of a 2.25 T magnetic field

H.G. Esser [a,*], A. Lyssoivan [b], M. Freisinger [a], R. Koch [b], G. Van Oost [b], F. Weschenfelder [a], J. Winter [a], TEXTOR- and ICRH-team [a,b]

[a] *Institut für Plasmaphysik, Forschungszentrum Jülich GmbH, Ass. EURATOM-KFA, D-52425 Jülich, Germany*

[b] *Laboratoire de Physique des Plasmas / Laboratorium voor Plasmafysica, Ass. Euratom-Belgian State, Ecole Royale Militaire / Koninklijke Militaire School, B-1000 Brussels, Belgium*

Abstract

To investigate *alternative conditioning concepts* for future fusion devices with permanent magnetic fields, plasmas produced by the coupling of ICRF power to He and gas mixtures of helium + silane, have been analyzed in the presence of a 2.25 T toroidal magnetic field at TEXTOR-94. Their qualification for wall conditioning has been investigated for different He-pressures, P_{He} $(1 \times 10^{-3} < P_{He}$ (Pa) $< 1 \times 10^{-1})$ and ICRF power, P_{ICRF} $(100 < P_{ICRF}$ (kW) $< 800)$. Electron densities n_e averaged along different radial lines of sight across the vacuum vessel from the top to the bottom have been obtained in the range $5 \times 10^{10} < n_e$ (cm^{-3}) $< 3 \times 10^{12}$. To study quantitatively the efficiency of hydrogen desorption from the first wall at different ICRF plasma conditions in a reproducible way, the first wall was presaturated by RG-glow discharges in H_2. The amount and the evolution of the H_2 desorption from rf discharge to rf discharge was determined by ion gauge measurements combined with mass spectrometry. To demonstrate the capability of the new method for plasma assisted thin film deposition, different amounts of silane (< 50%) were added to the He gas. During the ICRF pulses, the silane molecules were dissociated in the plasma and the Si atoms stick to the wall. A good balance of the amount of Si disappearing from the gas phase and that measured by post mortem surface analyses of collector probes at the wall position was found.

Keywords: TEXTOR; Wall pumping; Wall conditioning; Physical erosion; Desorption

1. Introduction and motivation

Wall cleaning and conditioning are considered as indispensable techniques in large fusion devices. They are not only important for the initial clean-down and start up of the machine but also between discharges to ensure reproducible and successful plasma break down and build-up of the main plasma current. Issues are impurity production and hydrogen desorption from surfaces loaded with hydrogen in previous discharges. These techniques may also be useful for controlling and reducing the tritium inventory of the device. DC-glow discharges are presently used in most cases to perform the wall conditioning of fusion devices. Well established conditioning processes, e.g. carbonization [1], boronization [2], or siliconization [3] are based on the dc-glow discharge technique. Presently it is essential as well for plasma assisted thin film deposition as for the bombardment of the first wall with energetic inert gas particles (e.g. helium) to desorb hydrogen. Glow discharges are not compatible with strong magnetic fields and hence not applicable in large future plasma devices (ITER, W7X, ...), which will have super-conducting coils and thus quasi permanent magnetic fields.

To explore alternative conditioning methods at TEXTOR-94, plasmas were produced by the coupling of ICRF power to helium and gas mixtures of helium + silane in the presence of a 2.25 T toroidal magnetic field. The experimental set up and the results achieved will be described and discussed in Section 2.

* Corresponding author. Tel.: +49-2461 61 5620; fax: +49-2461 61 2660; e-mail: h.g.esser@kfa-juelich.de

PII S0022-3115(96)00621-6

2. Experimental set up

The aims of the experiment were threefold:

- the production and characterization of ICRF plasmas under the given circumstances in TEXTOR-94;
- the investigation of the applicability of those plasmas for hydrogen desorption from first walls;
- the applicability of the new technique to layer deposition onto the first wall of TEXTOR-94.

2.1. The geometrical arrangement at TEXTOR-94

The geometry of TEXTOR-94 is characterized by 16 segments indicated by the numbers of the limiting magnetic coils (Fig. 1). Beside the gas handling system and the vacuum system, the ICRF system is the most important tool for these experiments. It comprises two double loop antennae, one (A1) without Faraday screen (FS), sector 2/3 the other (A2) with FS, sector 10/11, both antennae are optimized for plasma heating.

2.2. The ion cyclotron range of frequency (ICRF)

The ICRF wall conditioning technique is based on electron driven rf plasma production. To initiate the discharge, an antenna has to generate a rf electric field $\tilde{E}_{\|}$ parallel to magnetic field lines. According to theory [4,5], the rf field $\tilde{E}_{\|}$ at the rf antenna is responsible for neutral gas ionization by highly accelerated electrons during gas breakdown phase ($\omega > \omega_{pe}$, local ionization in the antenna area) and for excitation of plasma waves whose energy is absorbed by electrons during plasma build-up phase ($\omega \leq \omega_{pe}$, volume ionization all over the torus), whereby $\omega = 2\pi f$ is the rf frequency with f = rf generator frequency and ω_{pe} the electron plasma frequency $\omega_{pe} = (n_e e^2/\varepsilon_0 m_e)^{1/2}$, with n_e = electron density, e = electron charge, ε_0 = dielectric constant of the vacuum and m_e = electron mass. To optimize the ICRF plasma production process, antennae of different types, like frame [5,6], slot [4,6], Nagoya type-III [7] and 'crankshaft' [8] were developed. Experimental tests showed that standard ICRF antenna of loop type with and without Faraday screen (FS) as well may be also used for such purposes [9]. These antennae generate $\tilde{E}_{\|}$ the electrostatic rf field between the central conductor of the antenna and the side protection limiters.

To study the technical potential of ICRF discharges for wall conditioning purposes, the existing ICRF–TEXTOR system has been used. Being installed at toroidally opposite locations, the antennae were powered by separate rf generators. Each pair of the current straps in both antennae was fed either in phase (*zero*-phasing) or out-of phase (π-phasing) with typical total rf power (at generators) in the range ~ 100–800 kW with an antenna coupling efficiency of about 60%.

2.3. The gas (handling, vacuum system and analysis)

Helium (He) gas was used either pure or with different percentages of silane (SiH_4; SiD_4) for film deposition. The gas was filled into the TEXTOR vacuum vessel via the continuous gas inlet system with an even distributed and feedback controlled flow by three pipes with entries at the three sectors 5/6, 13/14 and 16/1.

The vacuum system of TEXTOR is equipped with 8 identical turbomolecular pumps (TP) distributed around the torus at every second sector starting with sector 1/2. The average of the pumping speed is about $S_{eff,He} = 320$

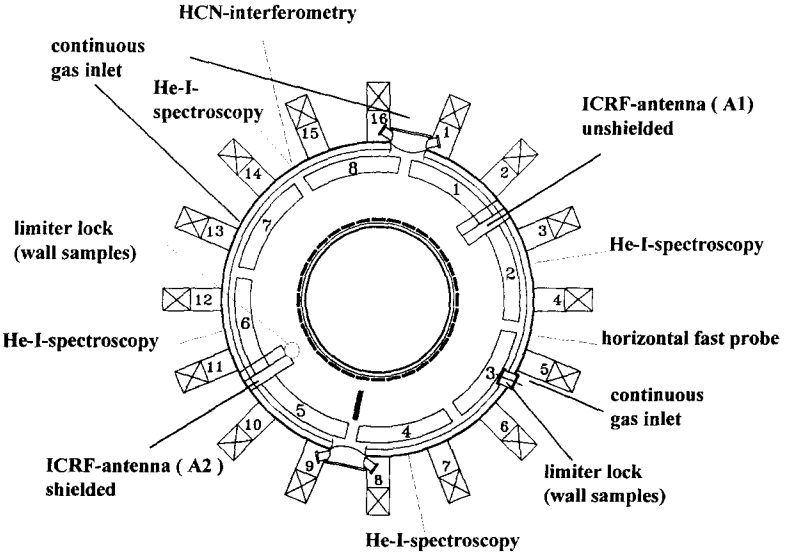

Fig. 1. Top view of TEXTOR 94, experimental set up and positions of diagnostics.

l/s for each pump in the molecular flow range. One additional TP with a pumping speed of about $S_{\mathrm{eff,He}} = 1900$ l/s is positioned at sector 8/9. It is mainly dedicated to the handling of reactive gases at TEXTOR. It is equipped with a thermal decomposer in the tubes of the forepump system, [10] to remove excessive reactive gas. During hydrogen desorption experiments 5 TP's were active with a total pumping speed for He of $S_{\mathrm{eff,He}} = 1570$ l/s.

Calibrated, stationary and dynamic measurements of gas pressures and partial pressures in the vacuum vessel provide the quantitative determination of the gas amounts entering and leaving the vessel for particle balance. The total pressure is measured by a fast ionization gauge in sector 8/9. Quadrupole mass spectrometers for the partial pressure measurements are placed in sector 9/10 and 16/1.

For reproducible investigations of hydrogen desorption, the wall, about 35 m^2, was preloaded with hydrogen in a glow discharge for 10 min in about 6×10^{-1} Pa pure H_2 and at average current density of 46 $\mu A/cm^2$. The wall temperature was typically 170°C ± 20°C. The outgassing time between the end of the glow and the first ICRF plasma in He was kept constant and was of the order of 10 min.

3. Results and discussion

3.1. Production and characterization of ICRF plasmas, $\omega \geq 2\omega_{CHe}$

3.1.1. ICRF plasma production in He

Reproducible and stable He-plasma production was obtained up to now in the parameter field of gas pressure and ICRF power as shown in the Fig. 2. Most of the experiments have been performed in the pressure range $1 \times 10^{-3} \leq P_{\mathrm{He}}$ (Pa) $\leq 1 \times 10^{-1}$ and ICRH power $100 \leq P_{\mathrm{ICRF}}$ (kW) ≤ 800. The toroidal magnetic field on axis was $B_{\mathrm{T}} = 2.25$ T.

Both antennae were excited simultaneously in time (A1 and A2 in π-phase) with rf pulses. The plotted electron density n_{eo} of the ICRF plasma in Fig. 2 are averaged values along the line of sight of the central channel of a HCN-interferometer in sector 14/15 radial, at different He pressures and coupled ICRF power. Plasmas with densities in the range $5 \times 10^{10} \leq n_{\mathrm{eo}}$ (cm^{-3}) $\leq 3 \times 10^{12}$ were obtained and the limits for ICRF plasma production have not yet been explored. The electron temperature (deduced from the ratio of the CI, CII and CIV line intensities observed in the plasma spectroscopic and electric probe measurements) was in the range 10–40 eV towards low pressure. Fig. 3 shows the evolution of 4 ICRF power pulses lasting each 1 s with 1 s in between. The ICRF power is increased by 100 kW pulse by pulse starting with 100 kW to 400 kW. The He pressure was $P_{\mathrm{He}} = 5 \times 10^{-3}$ Pa. The line averaged density profiles, deduced from the signals of the 9 channels HCN-interferometer, were centrally peaked. The peak electron density in the 400 kW plasma is 2×10^{11} cm^{-3}.

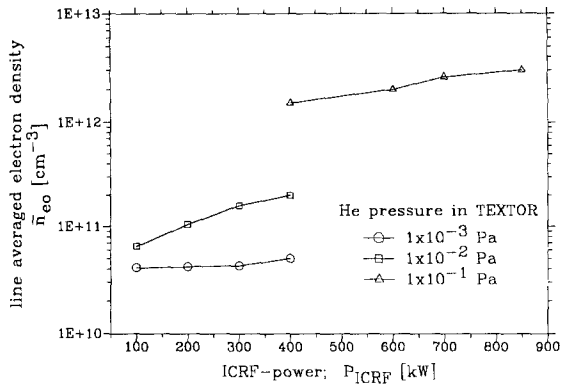

Fig. 2. Central line averaged electron density $\bar{n}_{\mathrm{eo}}$ as a function of ICRF power at the generators for different He-pressures in TEXTOR during ICRF plasma production.

A bright vertical column of light emission in the vicinity of the 2nd harmonic layer was observed from CCD camera looking tangential at the plasma in the antenna A2 area. With B_{T} ramping down, the vertical column followed the 2nd harmonic layer and was clearly seen to be shifted to the high field side. In this frequency range, the slow wave is strongly evanescent and the power is expected to be mostly collisionally dissipated in the ion Bernstein wave, coupling taking place directly at the antenna or at the 2nd cyclotron harmonic layer. The observed phenomena may be attributed to increased energy dissipation near the 2nd harmonic layer.

3.1.2. Multi-ion species rf plasma production (helium + silane)

Two different types of behaviour of rf discharges have been observed depending on the silane concentration. In the case of normal silane (SiH_4), ICRF discharge was only possible with small ($\leq 10\%$) concentrations of the reactive gas. The averaged electron density did not exceed the value 10^{12} cm^{-3} because of strongly decreased antenna-plasma coupling and high rf power reflection increasing as the SiH_4 concentrations rise.

Using deuterated silane (SiD_4), ICRF discharges in gas mixture of 50% (^{4}He) and 50% (SiD_4) have been realized for the first time and the concentration of 50% was not observed as upper limit.

3.2. Hydrogen desorption

To investigate the applicability of ICRF plasma concerning hydrogen desorption, the first wall was prefilled with hydrogen as described above and ICRF-He plasma was ignited in the vessel. The temperature of the first wall during the experiment was almost at about 170°C and the He-pressure at the beginning of the ignition of the ICRF

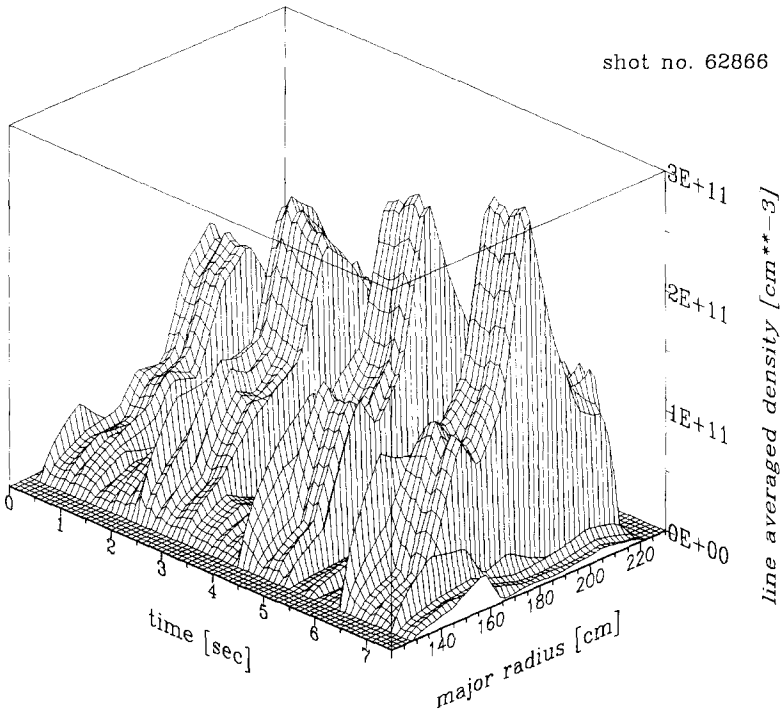

Fig. 3. 3D plot of the temporal evolution of the line averaged electron density $\bar{n}_e(R)$ of a pulsed ICRF plasma; 4 pulses, 1 s each and 1 s in between; increase of the ICRF-power by 100 kW from pulse to pulse starting with 100 kW in the first pulse.

plasmas was about 5.5×10^{-3} Pa. Fig. 4 shows the temporal evolution of the calibrated signals of the total pressure of 5 successive plasma discharges (#50–#54) each consisting of 4 pulses of 1 s duration and 1 s in between. The ICRF power was 200 kW per antenna for each pulse as can be seen on the right hand scale of the plot. The integral of the total pressure of each plasma discharge corrected for the base pressure due to the still flowing He gas, represents the amount of the desorbed gas, coming from the wall after the ICRF plasma pulses. Measurement with the quadrupole mass spectrometer confirmed that more than 90% of the pressure raise was due to hydrogen.

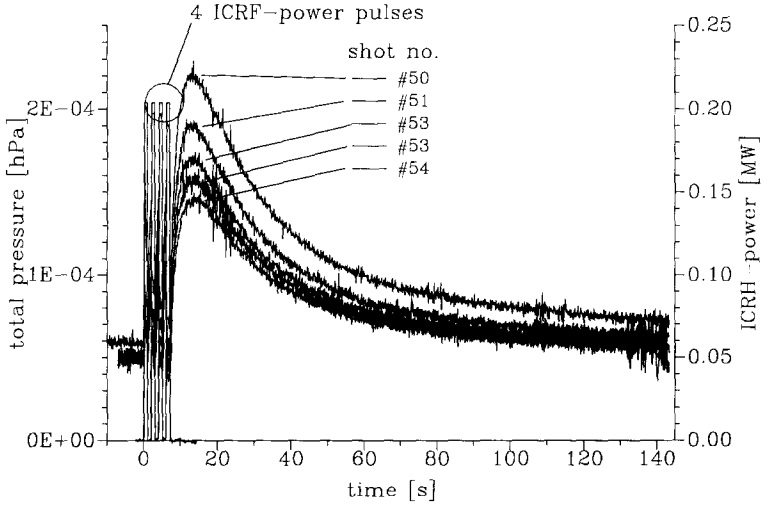

Fig. 4. Measurement of the desorbed gas (mainly H_2) by 5 successive ICRF-He-plasmas in TEXTOR; total pressure as function of time; wall (liner) temperature 180°C.

The total amount of desorbed H_2 is decreasing discharge by discharge, see curves of the total pressure for the shots #50 to #54 in Fig. 4, due to the successive depletion of the hydrogen content in the near surface region of the first wall. Fig. 5 shows the decrease of the integrated amount of the desorbed gas of the 5 successive ICRF plasma discharges.

The total amount of the desorbed gas is of the order of 1.2 Pa m^3 (6.5×10^{20} H-atoms) which corresponds to ~ 1 monolayer of the whole inner wall area supposed homogeneous. This is compatible with the small range of the He-ions of several eV energy. For comparison, the content of H atoms in a TEXTOR discharge with an electron density of $n_{e,tot} = 4 \times 10^{13}$ cm^{-3} is of the order of 1.5×10^{20} atoms.

3.3. Layer deposition studies (LDS)

To demonstrate the possibility of layer deposition by ICRF plasma with reactive gases, silane was added to the He gas as described above. Dynamical investigations of gas partial pressures by mass spectrometer measurement before, during and after the ICRF plasma discharges show, that the silane disappears to a large fraction from the residual gas immediately after the ignition of the ICRF plasma as can be seen in Fig. 6.

The masses 30 and 31 representing the ion fragments SiH_2 and SiH_3 of silane drop to a large extend and recover the original value due to continuous gas filling of the He/SiH_4 mixture with the typical gas filling constant of the TEXTOR vacuum vessel. The silane molecules are ionized in the ICRF plasma, hit the wall and stick there, building a layer.

Post mortem surface analysis by EPMA (electron probe micro analyses) of wall samples inserted at two different wall positions in the TEXTOR sectors 5/6 and 10/11 verify the deposition of silane. About 1.2×10^{15} Si atoms/cm^2 were found at the sample in sector 10/11 close to the ICRF antenna and in sector 5/6 between both antennae, 7×10^{14} Si atoms/cm^2 were found. The total exposure time of the samples to ICRF plasma was about 17 s. The deposition rate is of the same order compared to the deposition rate in RG glow discharges which is typically of the order of 1 monolayer/min. The homogeneity of the deposition has to be studied in more detail, nevertheless, first measurements reveal variation in layer thickness of about a factor of 2, similar to RG-glow discharges. Thus the ICRF plasma efficiency for layer deposition is comparable to RG-glow discharges.

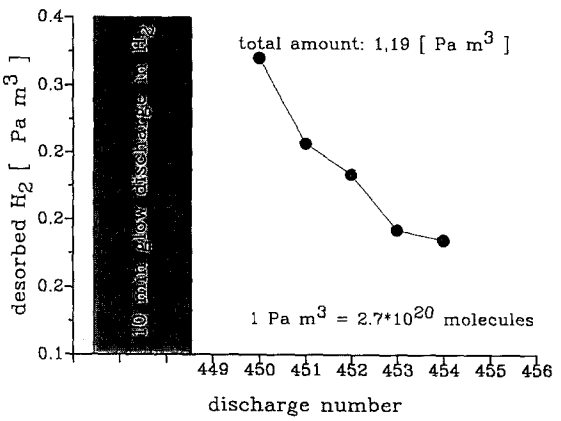

Fig. 5. Successive decrease of the amount of H_2 desorbed from a H_2 preloaded first wall of TEXTOR by ICRF-He-plasmas; wall (liner) temperature 180°C.

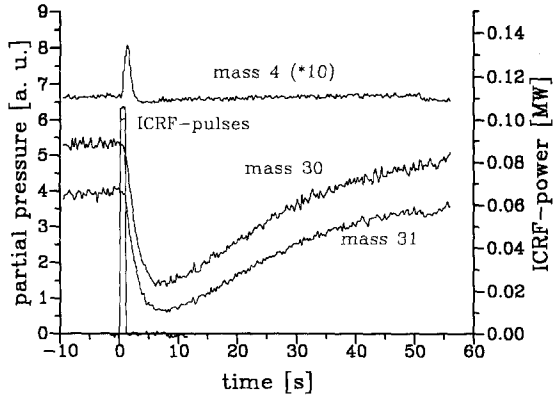

Fig. 6. Temporal evolution of the silane partial pressure indicated by the fragment ion values 30 and 31 before, during and after a 1 s ICRF power pulse of about 200 kW.

4. Summary and conclusions

ICRF-conditioning has been successfully tested in TEXTOR-94 as at Tore Supra [11]. This technique is applicable in presence of magnetic fields and thus applicable in future large devices with superconducting coils.

The ICRF-conditioning is based on He plasma production by application of rf power in the ion cyclotron frequency range at 32.5 MHz in the presence of a magnetic field B_T of 2.25 T. The antennae used in TEXTOR-94, one with the other without Faraday shield.

A scenario for reliable ICRF plasma production was identified and characterized. The present parameter field (ICRF power 100 kW up to 800 kW) and gas pressures (1×10^{-3} Pa to 1×10^{-1} Pa) for plasma production is not yet completely explored.

First results on hydrogen desorption from the first wall and on ICRF plasma assisted layer deposition in a helium silane mixture were obtained.

The layer deposition efficiency of the new method is similar to standard technique using RG glow discharge already now. It will be attempted in future experiments to heat the ions as to increase the rate and total amount of

hydrogen desorption beyond the equivalent of 1 monolayer which is observed at present.

The efficiency of hydrogen desorption in permanent magnetic field has already been demonstrated in Tore Supra [11]. The demonstration of conditioning layer deposition is planned in cooperation also with Tore Supra. Still open questions are a detailed characterization of the plasma and the homogeneity of the conditioning effect to the first wall. The development of optimized antenna to increase the power coupling to the ICRF plasma (energy of the ions) may turn out to be important for an optimized setup.

Acknowledgements

The authors wish to acknowledge the support of the TEXTOR operating team. In particular we want to thank H. Reimer for preparing and handling the gas and vacuum systems and F. Durodié and M. Vervier for the operation of the ICRH system and J. Boedo for Langmuir probe measurements.

References

[1] J. Winter, J. Nucl. Mater. 145–147 (1987) 131.
[2] J. Winter et al., J. Nucl. Mater. 162–164 (1989) 713.
[3] J. Winter, Phys. Rev. Lett. 71 (1993) 1549.
[4] A.I. Lyssoivan et al., Nucl. Fusion 32(8) (1992) 1361.
[5] O.M. Shvets et al., Proc. 4th Int. Symp. on Heating in Toroidal Plasmas, Roma, Vol. 1 (1984).
[6] O.M. Shvets et al., Nucl. Fusion 26(11) (1986) 23.
[7] K. Nishimura et al., Proc. 7th Int. Workshop on Stellarators, IAEA, Vienna (1990) p. 265.
[8] V.E. Moiseenko et al, Proc. 21st EPS Conf. on CFPP, Montpellier 1994, Vol. 18B, Part 2 (1994) p. 980.
[9] A.I. Lyssoivan et al., Proc. 22nd EPS Conf. on CFPP, Bournemouth, Vol. 19C, Part (1995).
[10] H.G. Esser et al., Fusion Technol. 1 (1988) 791.
[11] E. Gauthier, these Proceedings, p. 553.